Catalysis and Stability of Triosephosphate Isomerase from *Trypanosoma brucei* with Different Residues at Position 14 of the Dimer Interface. Characterization of a Catalytically Competent Monomeric Enzyme†

Gloria Hernández-Alcántara,‡ Georgina Garza-Ramos,§ Guillermo Mendoza Hernández,§ Armando Gómez-Puyou,‡ and Ruy Pérez-Montfort*,‡

Departamento de Bioquímica, Instituto de Fisiología Celular Universidad Nacional Autónoma de México, Apartado Postal 70242, 04510 México DF, México, and Departamento de Bioquímica Facultad de Medicina Universidad Nacional Autónoma de México, 04510 México DF, México

Received October 18, 2001

ABSTRACT: In homodimeric triosephosphate isomerase from *Trypanosoma brucei* (TbTIM), cysteine 14 of each the two subunits forms part of the dimer interface. This residue is central for the catalysis and stability of TbTIM. Cys14 was changed to the other 19 amino acids to determine the characteristics that the residue must have to yield catalytically competent stable enzymes. C14A, C14S, C14P, C14T, and C14V TbTIMs were essentially wild type in activity and stability. Mutants with Asn, Arg, and Gly had low activities and stabilities. The other mutants had less than 1% of the activity of TbTIM. One of the latter enzymes (C14F) was purified to homogeneity. Size exclusion chromatography and equilibrium sedimentation studies showed that C14F TbTIM is a monomer, with a k_{cat} ∼1000 times lower and a K_m ∼6 times higher than those of TbTIM. In C14F TbTIM, the ratio of the elimination (methylglyoxal and phosphate formation) to isomerization reactions was higher than in TbTIM. Its secondary structure was very similar to that of TbTIM; however, the quantum yield of its aromatic residues was lower. The analysis of the data with the 19 mutants showed that to yield enzymes similar to the wild type, the residue must have low polarity and a van der Waals volume between 65 and 110 Å^3. The results with C14F TbTIM illustrate that the secondary structure of TbTIM can be formed in the absence of intersubunit contacts, and that it has sufficient tertiary structure to support catalysis.

Triosephosphate isomerase (TIM,[1] EC 5.3.1.1) is a glycolytic enzyme that catalyzes the interconversion between dihydroxyacetone phosphate (DHAP) and D-glyceraldehyde 3-phosphate (GAP) (*1*). At present, more than 100 amino acid sequences of TIMs from a variety of organism are available in the databases and the X-ray structures of TIMs from 12 different species have been determined (*2*−*13*). Except for TIMs from thermophilic organisms, which are tetramers (*12*, *13*), all TIMs are composed of two identical subunits. These subunits associate through noncovalent interactions to form a homodimer with a high association constant. The monomers are formed by eight central β-strands and eight α-helices (numbered 1−8) joined by loops, making TIM a member of the protein family with the $(\beta\alpha)_8$ barrel fold. Each monomer contains all the residues that participate in catalysis. Nonetheless, a well-documented property of TIM is that it is catalytically active only in its dimeric form (*14*, *15*).

In all TIMs, the area of the dimer interface comprises a large portion of the enzyme. For example, in TIM from *Trypanosoma brucei* (TbTIM), the area of contact between the two monomers is approximately 1600 Å^2 (*4*). The dimer interface is formed mainly by loops 1−4. The protruding loop 3 of one subunit docks into a deep pocket formed by loops 1 and 4 of the other subunit and is near the catalytic site. Cys14 in loop 1 is one of the three residues that are fully exposed in the monomer and completely buried in the TbTIM dimer (Figure 1); the other two are Val46 and Thr75 that are in loop 2 and loop 3, respectively. The side chain of Cys14 is surrounded by the residues of loop 3 of the other subunit (Figure 1), which is consistent with data that indicate that the pK_a of the −SH group of the interface Cys14 is higher than that of the same group of the amino acid in solution (*16*). In the crystallographic structure of TbTIM, the side chain of Cys14 is hydrogen-bonded to Gly72 of the other subunit, and less than 0.38 nm from Ser71, Glu77, Val78, and Ser79 of loop 3 of the other monomer (*17*).

The residue at position 14 is a nonconserved amino acid. In TIMs from some pathogenic parasites, residue 14 is Cys, whereas in TIMs from other species, including *Homo sapiens*, position 14 is occupied by a different amino acid,

† Supported by DGAPA-UNAM Grant IN-200600 and CONACyT Grant G27551M. G.H.-A. is the recipient of a fellowship from CONACyT.

* To whom correspondence should be addressed. Telephone: (52) 55 56225657. Fax: (52) 55 56225630. E-mail: rmontfor@ifisiol.unam.mx.

‡ Instituto de Fisiología Celular Universidad Nacional Autónoma de México.

§ Departamento de Bioquímica Facultad de Medicina Universidad Nacional Autónoma de México.

[1] Abbreviations: CD, circular dichroism; DHAP, dihydroxyacetone phosphate; GAP, D-glyceraldehyde 3-phosphate; M_r, relative molecular mass; PCR, polymerase chain reaction; SCM, spectral center of mass; R_s, Stokes radius; TEA, triethanolamine; TIM, triosephosphate isomerase; TbTIM, triosephosphate isomerase from *T. brucei*.

10.1021/bi011950f CCC: $22.00
Published on Web 03/07/2002

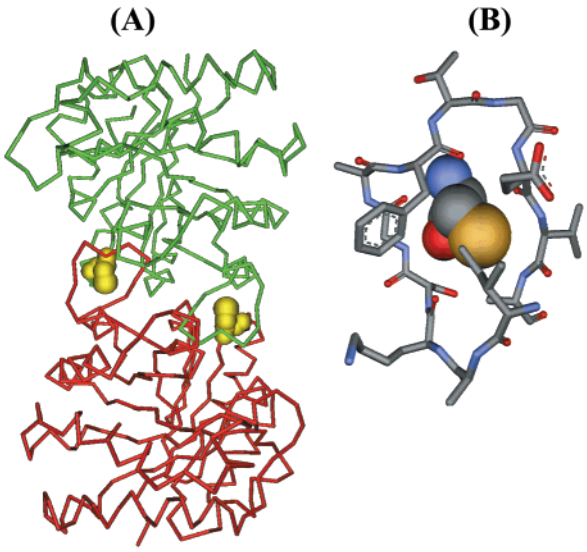

FIGURE 1: Relative position of Cys14 and the subunits of TbTIM (A) and packing of Cys14 of one subunit with the residues of loop 3 from the other subunit (B). (A) The α-carbon traces of subunits A and B are shown in red and green, respectively, and a CPK depiction of Cys14 from both subunits is shown in yellow. (B) Cys14 is shown as a CPK image, and the residues of loop 3 from the other subunit are shown as sticks. The color coding for the elements is as follows: gray for H and C, blue for N, red for O, and yellow for S. The three-dimensional coordinates are from PDB entry 5TIM.

the most common being Met and Leu, followed by Ser, Thr, Gln, and Ala. In TbTIM and TIMs from *T. cruzi* and *Leishmania mexicana*, Cys14 is the only cysteine that forms part of their dimer interfaces. The incubation of the trypanosomal enzymes with sulfhydryl reagents brings about large structural changes and abolition of catalysis, which results from the derivatization of Cys14 by the sulfhydryl reagents (*17*, *18*). In addition to trypanosomal TIMs, the pathogenic parasites *Entamoeba histolytica* (*19*), *Plasmodium falciparum* (*20*), and *Giardia lamblia* (*21*) have the interface Cys. Therefore, this region of the interface has received considerable attention as a potential target for the design of drugs that specifically perturb the association between monomers of the parasite enzymes (*17*, *18*, *22*, *23*).

In this work, we have further studied the contribution of Cys14 to the stability and activity of TbTIM. We performed exhaustive mutagenesis of Cys14 of TbTIM to investigate which amino acids can replace the interface Cys and, thus, establish the characteristics that an amino acid in that position must have to yield catalytically competent enzymes. Only a limited number of mutant enzymes exhibited activities and stabilities similar to those of wild-type TbTIM. We also found that a point mutation, the substitution of Cys14 with Phe, yields a stable monomeric variant of TbTIM that exhibits substantial catalytic activity.

MATERIALS AND METHODS

Construction of the Cys14 Mutants. The substitution of Cys at position 14 with the other 19 amino acids in TbTIM was accomplished with the polymerase chain reaction (PCR) using the Expand High Fidelity PCR System (Boehringer). The mutagenic oligonucleotides were 5′AACTGGAAGNNNAACGGCTCC3′ [C14V, C14F, C14L, C14S, C14Y, C14P, and C14K forward (Fw)] and 5′GGAGCCGTTNNNCTTCCAGTT3′ [C14V, C14F, C14L, C14S, C14Y, C14P, and C14K reverse (Rv)] (where N is A, C, G, or T), 5′AACTGGAAGVVNAACGGCTCC3′ (C14T, C14H, C14Q, C14N, C14D, C14E, C14R, and C14G Fw) and 5′GGAGCCGTTNBBCTTCCAGTT3′ (C14T, C14H, C14Q, C14N, C14D, C14E, C14R, and C14G Rv) (where V is A, C, or G and B is T, G, or C), 5′AACTGGAAGGCGAACGGCTCC3′ (C14A Fw) and 5′GGAGCCGTTCGCCTTCCAGTT3′ (C14A Rv), 5′AACTGGAAGATCAACGGCTCC3′ (C14I Fw) and 5′GGAGCCGTTGATCTTCCAGTT3′ (C14I Rv), and 5′AACTGGAAGTGGAACGGCTCC3′ (C14W Fw) and 5′GGAGCCGTTCCACTTCCAGTT3′ (C14W Rv). The external oligonucleotides were the T7 promoter and T7 terminator (Novagen). The respective mutations were introduced as follows: 30 cycles for 1 min at 94 °C, 1 min at 55 °C, and 1 min at 72 °C and incubation for 10 min at 72 °C. The genes were cloned in the pCR 2.1 vector (Invitrogen) and sequenced. Once the genes with the appropriate mutation were identified, they were sequenced completely, subcloned into the pET-3a expression vector as *Nde*I fragments, and introduced by transformation into BL21(DE3)pLysS cells (Novagen).

Growth of the Cells and Protein Expression. For expression of the mutant proteins, cells were grown at 37 °C in Luria-Bertani medium supplemented with 100 μg/mL ampicillin and 34 μg/mL chloramphenicol. When cultures reached an A_{600} of 0.6, isopropyl β-D-thiogalactopyranoside at a final concentration of 0.4 mM was added. Growth was continued overnight at 37 °C for cells with wild-type TbTIM and the C14V mutant, or at 30 °C for the rest of the mutants. BL21(DE3)pLysS cells transformed with C14F and C14K were induced at 21 °C. The growth of the cells containing the C14F mutant was continued for 3 h.

Purification of Enzymes. Cultures (250 mL) were collected by centrifugation and suspended in 10 mL of cell lysis buffer (25 mM Mes/NaOH) (pH 6.5), 1 mM dithiothreitol, 1 mM EDTA, and 0.2 mM phenylmethanesulfonyl fluoride. The suspensions were sonicated (five intervals of 45 s) and centrifuged at 15 000 rpm for 15 min. The pellet was suspended in lysis buffer, which in addition had 200 mM NaCl, gently stirred on ice for 30 min, and centrifuged for 15 min at 15 000 rpm (*24*). The latter supernatant was used for an assay of activity and for determining the relative abundance of TIM concentration by SDS−PAGE analysis, Coomassie blue staining, and densitometry.

The purification of wild-type TbTIM and the mutants C14A, C14P, C14S, C14T, C14V, and C14G was carried out following the methodology described by Borchert et al. (*24*). The C14F mutant was purified as follows. Cells were lysed by passing them three times through a French press in 25 mM Mes/NaOH (pH 6.5), 1 mM dithiothreitol, 1 mM EDTA, and 0.2 mM phenylmethanesulfonyl fluoride. The lysate was centrifuged at 15 000 rpm for 15 min. The pellet was suspended in lysis buffer with 200 mM NaCl, stirred at 4 °C for 18 h, and centrifuged at 15 000 rpm for 15 min. The supernatant was dialyzed exhaustively against 25 mM triethanolamine (TEA) (pH 8.0), 1 mM EDTA, 1 mM dithiothreitol, and 1 mM sodium azide. The protein was loaded onto a carboxymethyl-Sepharose fast flow column, equilibrated with the same buffer. Protein was eluted with a gradient of 0 to 150 mM NaCl. In all the steps of the purification, catalytic activity and SDS−PAGE analysis using

Coomassie blue staining and densitometry were carried out. C14N was only partially purified. For this enzyme, we followed the procedure (*24*) up to the step in which it was precipitated with ammonium sulfate.

Activity Assays. Enzyme activity was determined at 25 °C by following the decrease in absorbance at 340 nm of a mixture that contained 100 mM TEA and 10 mM EDTA (pH 7.4), 1 mM GAP, 0.2 mM NADH, and glycerol-3-phosphate dehydrogenase (20 μg/mL). Except where specified, the reaction was initiated by the addition of TIM at the indicated concentration (*25*). For the determination of K_m and V_{max}, the concentration of GAP was varied over a concentration range of 0.06−2 mM. The K_m and V_{max}, in the direction of DHAP to GAP, were determined at 25 °C in a mixture of 0.2 mL that contained 100 mM TEA, 10 mM EDTA (pH 7.4), 1 mM NAD, 4 mM arsenate, 120 μM dithiothreitol, 1 unit of GAP dehydrogenase, and 0.3−10 mM DHAP.

Methylglyoxal Formation. Methylglyoxal formation was monitored at a single substrate concentration using the method of Richard (*26*). The enzyme concentration was 18 μM, and the [^{32}P]DHAP concentration was 0.5 μM. Time points were collected over the course of 20 h.

Stability to Dilution. Different concentrations of TbTIM mutants were incubated for 24 h at 25 °C in 100 mM TEA and 10 mM EDTA (pH 7.4). The catalytic activity was measured by adding an aliquot of the sample to the reaction mixture, yielding a final enzyme concentration of 5 ng/mL. The curves of remaining activity versus protein concentration were used to calculate the dissociation constant (K_d) of the wild type and five mutants according to the formulations derived by Mainfroid et al. (*27*). The following equation was used to calculate the K_d:

$$\mathrm{SpA} = \mathrm{SpA}_{max}[4E_0 + K_d - (8E_0K_d + K_d^2)^{1/2}]/4E_0 \quad (1)$$

where SpA is the specific activity, SpA_{max} the maximum specific activity, and E_0 the total monomer concentration. This model assumes that the dimer is the only active species.

Circular Dichroism Spectroscopy. Circular dichroism (CD) spectra were obtained at 25 °C with an AVIV (Lakewood, NJ) 62 HDS spectropolarimeter. The quartz cells had path lengths of 0.1 and 1.0 cm for measurements in the far-UV and near-UV regions, respectively. For determination of the spectra, solutions of the enzymes were equilibrated against a 25 mM phosphate buffer (pH 7.4) containing 20 mM NaCl. Each spectrum was the average of five repetitive scans and was corrected by subtracting the average spectrum of the buffer.

Thermal Unfolding. Thermal denaturation of the enzymes was assessed by recording protein ellipticity at 222 nm in the range between 20 and 70 °C. The temperature of the samples was increased at a rate of 1 °C/2.5 min. For the experiments, proteins (400 μg/mL) were previously dialyzed against a 20 mM MOPS buffer (pH 7.0) that included 1 mM EDTA, 1 mM dithiothreitol, and 1 mM azide. Denaturation was irreversible in all samples. From the data, the apparent fraction of denatured subunits (f_D) was calculated using the equation

$$f_D = (y_N - y)/(y_N - y_D) \quad (2)$$

where y_N and y_D are the ellipticity values characteristic of the native and unfolded subunits, respectively. The two parameters were linear extrapolations from the initial and final portions of the curve of y versus temperature.

Fluorescence Measurements. The emission fluorescence spectra of wild-type TbTIM and C14F TbTIM were recorded between 300 and 400 nm at an excitation wavelength of 280 nm with a Shimadzu RF-5000U spectrofluorometer. Their protein concentration was 50 μg/mL in 100 mM TEA and 10 mM EDTA (pH 7.4). The spectrum of the buffer was subtracted from the experimental. The spectral center of mass (SCM) of each spectrum was calculated according to the equation

$$\mathrm{SCM} = \sum \lambda I(\lambda) / \sum \mathrm{I}(\lambda) \quad (3)$$

where $I(\lambda)$ is the fluorescence intensity at wavelength λ.

Molecular-Sieve Chromatography. The oligomeric state of C14F was studied by zone size exclusion chromatography using a Beckman HPLC system with a 7.5 mm × 300 mm UltraSpherogel-SEC 3000 column, with a pore size of 230 Å [relative molecular mass (M_r) range of 5×10^3 to 7×10^5 Da]. The mobile phase contained 100 mM sodium phosphate (pH 7. 0), 1 mM EDTA, and 150 mM NaCl. Before injection, samples were filtered through a 0.22 μm filter and eluted at a flow rate of 1 mL/min. The protein profile was monitored at 280 nm. Stokes radius (R_s) determinations were performed using well-characterized globular protein standards with known R_s values as described by Ackers (*28*). For comparison, wild-type TbTIM was also analyzed.

Sedimentation Analysis. Experiments were performed using an analytical ultracentrifuge equipped with scanner optics (Optima model XL-A, Beckman, Fullerton, CA). The protein sample solution was exhaustively dialyzed at 4 °C against 0.1 M TEA-HCl buffer (pH 7.4) that contained 1 mM dithiothreitol and 10 mM EDTA. A portion of the dialysate was retained and used as the reference solution. The protein samples were placed in cells fitted with conventional aluminum-filled Epon double-sector centerpieces and quartz windows. Sedimentation velocity experiments at an enzyme concentration of 0.4 mg/mL were performed at 40 000 rpm. The sedimentation coefficient was corrected for temperature (20 °C) and water viscosity (ν_p = 0.7468 mL/g, ρ_o = 1.019 g/mL). The scans were analyzed using the SVEDBERG data analysis software (Amgen, Inc.) developed by Philo (*29*). Sedimentation equilibrium experiments were carried out at 15 000 and 18 000 rpm at 20 °C. Scans were taken at 280 nm, with a spacing of 0.001 cm, in a step scan mode at intervals of 4 h. Sedimentation equilibrium was judged to have been reached when the difference in concentration distributions between consecutive scans was zero. Data sets were analyzed using the nonlinear regression program NONLIN (*30*). The program fits to a reduced apparent molecular mass, via the relation $\sigma = [M(1 - \upsilon\rho)\omega^2]/(RT)$, where M is the molecular mass, υ is the partial specific volume, ρ is the solvent density, ω is the radial velocity, R is the gas constant, and T is the absolute temperature (kelvin).

Other Assays. Protein concentrations of the enzymes were determined with the BCA Protein Assay Kit (Pierce) and

Table 1: Specific Activities and Relative Abundance of Wild Type TbTIM and the 19 Cys14 Mutants[a]

	specific activity (units/mg)	relative abundance (%)
wild type	2858	100
C14T	3680	105
C14A	3624	99
C14P	2575	99
C14V	2531	94
C14S	2583	85
C14N	556	85
C14R	537	83
C14G	157	86
C14F	23	69
C14K	22	32
C14D	18	54
C14H	6	35
C14E	6	44
C14I	6	46
C14W	6	17
C14Y	5	50
C14Q	4	50
C14L	2	26
C14M	1	23

[a] Activity and protein were measured in the supernatant obtained after salt extraction of the particulate fraction (see Materials and Methods). The specific activities are shown. The relative abundance of the enzymes was calculated after scanning SDS−PAGE gels stained with Coomassie blue. The gels were loaded with 10 μg of protein. The intensity of the band obtained with wild-type TbTIM was considered 100%. Note that the abundance of some enzymes, particularly those with low activity, was significantly lower than in the control. However, the lower abundance would not account for their very low levels of specific activity.

by their absorbance at 280 nm using a molecular extinction coefficient (ϵ_{280}) of 34 950 M^{-1} cm^{-1} (*22*).

RESULTS

Cys14 of TbTIM was exhaustively substituted by site-directed mutagenesis. All 19 mutant enzymes were cloned and expressed in *Escherichia coli.* The initial steps of purification of wild-type TbTIM involve centrifugation of the cell lysate, and extraction of the enzyme from the particulate fraction with buffer that has a high salt concentration (*24*). We followed this procedure with all proteins. Their specific activities and relative abundance are shown in Table 1. The latter was inferred from Coomassie blue staining of SDS gels loaded with 10 μg of protein. Five mutants (T, A, P, V, and S) had essentially wild-type activity; these will be termed "high-activity mutants". Three mutants (N, R, and G) exhibited between 10 and 20% of the specific activity of wild-type TbTIM. The remaining 11 mutants exhibited activities of less than 1% of the wild-type activity (Table 1). It is noted that, at this stage of purification, the activity traces of mutants C14N, C14R, and C14G were not linear; instead, there was a progressive decay of activity during the time of recording. The activities shown correspond to those observed in the first minute of the reaction (see below).

Purification of the High-Activity Mutants, C14G TbTIM, and C14F TbTIM. We purified to homogeneity and characterized all the high-activity mutants and one of the mutants (C14G) with intermediate activity. The yield of these enzymes was similar to that of the wild type (60−80 mg/L of culture). We also purified C14F TbTIM (one of the mutants with low activity) to homogeneity. After purification, all the previous enzymes exhibited a single protein band in SDS gels loaded with 10 μg of protein and stained with Coomassie blue (data not shown). Due to the tendency of C14F TbTIM to aggregate, the purification required some modifications of the standard method (see Materials and Methods) and the yield was ∼90% lower. One feature of this mutant is that it underwent aggregation at concentrations higher than 2 mg/mL. C14N TbTIM was purified up to the step in which it is precipitated with 65% saturation ammonium sulfate. We attempted to purify the C14M and C14L enzymes, but we were unsuccessful; the enzymes exhibited a strong tendency to undergo aggregation.

Table 2: Kinetic Constants of Wild-Type TbTIM and the Indicated Cys14 Mutants[a]

	$K_{m(GAP)}$ (mM)	$k_{cat(GAP)}$ (min^{-1})	$K_{m(DHAP)}$ (mM)	$k_{cat(DHAP)}$ (min^{-1})
wild type	0.35 ± 0.05	$(2.6 \pm 0.13) \times 10^5$	1.9	2.7×10^4
C14A	0.43	3.1×10^5	1.7	2.8×10^4
C14P	0.33	2.2×10^5	1.1	2.2×10^4
C14S	0.5	3.0×10^5	1.9	2.8×10^4
C14T	0.32	2.3×10^5	1.3	1.4×10^4
C14V	0.42	2.4×10^5	1.5	2.5×10^4
C14F	3.6 ± 1.3	114 ± 23	5.2	9

[a] The measurements were made with dihydroxyacetone phosphate (DHAP) in the range of 0.325−10 mM; for glyceraldehyde 3-phosphate (GAP), the substrate concentrations were between 0.06 and 2 mM. The reaction was started by addition of the enzyme. With all enzymes, except C14F, 100 ng/mL was used in the direction of DHAP to GAP and 5 ng/mL in the opposite direction; with C14F, the reactions were assayed with 100 and 200 μg/mL enzyme, respectively. K_m and k_{cat} were calculated from nonlinear regression plots. The values for the C14A, C14P, C14S, C14T, and C14V mutants in the direction of GAP to DHAP are the average of two experiments, and the values of K_m and k_{cat} differed by less than 10%. With DHAP as the substrate, only one experiment was carried out. For the wild type, we took the average of five different preparations ± standard error; the data for C14F are the average of four experiments ± standard error.

Kinetic Properties of Mutant Enzymes. The steady-state kinetics of the wild type and the high-activity mutants were determined in the forward (DHAP to GAP) and backward (GAP to DHAP) directions (Table 2). With the two substrates, the K_m and k_{cat} values of TbTIM and the high-activity mutants were strikingly similar. In the C14F mutant, the catalytic constants in the forward and backward directions were ∼3000- and ∼1000-fold lower than in wild-type TbTIM, respectively; the K_m values for GAP and DHAP were 6 and 3 times higher, respectively, than in the wild type. The K_i value for the competitive inhibitor 2-phosphoglycolate was nearly 3 times higher in C14F TbTIM ($K_i = 0.076 \pm 0.008$ mM) than in wild-type TbTIM ($K_i = 0.024$ mM).

With the wild type and the C14A, C14P, C14S, C14T, and C14V mutants, the activity traces with 5 ng of protein were linear. The same linearity was observed with C14F; it is noted that due to the low activity of this enzyme, microgram quantities were used for activity assays (Table 2). On the other hand, the C14G and C14N mutants exhibited a progressive decay of activity during the time of recording. The experiments shown in Figure 2 illustrate this behavior. Mutants C14G and C14N were incubated at concentrations of 1.3 and 0.05 μg/mL, respectively. At different times, the coupling enzyme and substrate were added to initiate catalysis. With C14G, ∼15% of the activity remained after incubation for 2 min. With C14N, an incubation of 1 min sufficed to induce almost total abolition of activity. This

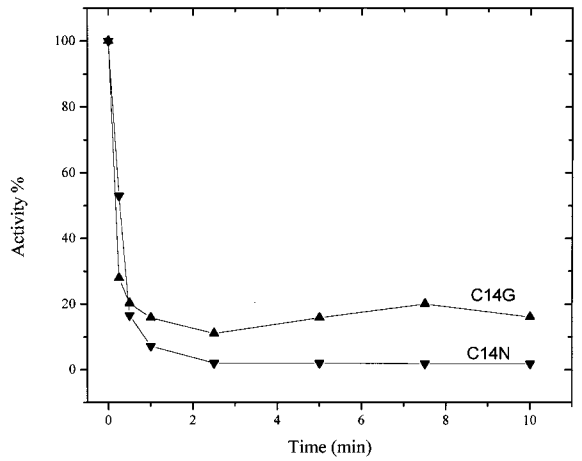

FIGURE 2: Inactivation of C14G and C14N TbTIMs. C14G and C14N had been stored at concentrations of 1.3 and 1.5 mg/mL, respectively. At the time of the experiments, 1.3 μg of C14G TbTIM or 0.05 μg of C14N TbTIM was introduced into spectrophotometer cells that contained 1 mL of 100 mM TEA and 10 mM EDTA (pH 7.4). At the indicated times, the reagents required for assay of activity (GAP, NADH, and α-glycerophosphate dehydrogenase) were added and activity was recorded. The data that are shown correspond to the first minute of reaction time. The results are expressed as a percentage of activity; 100% corresponds to the activity observed when the enzymes were introduced to the complete reaction mixtures. The 100% values were 27.2 and 670.5 μmol min^{-1} mg^{-1} for the C14G and C14N mutants, respectively. With wild-type TbTIM, no significant changes in activity were detected after its incubation for 10 min at a concentration of 5 ng/mL (4027 μmol min^{-1} mg^{-1}). Note that the C14G mutant that was used had been purified to homogeneity and that C14N TbTIM had only been purified up to the step in which it was precipitated with 65% saturation ammonium sulfate.

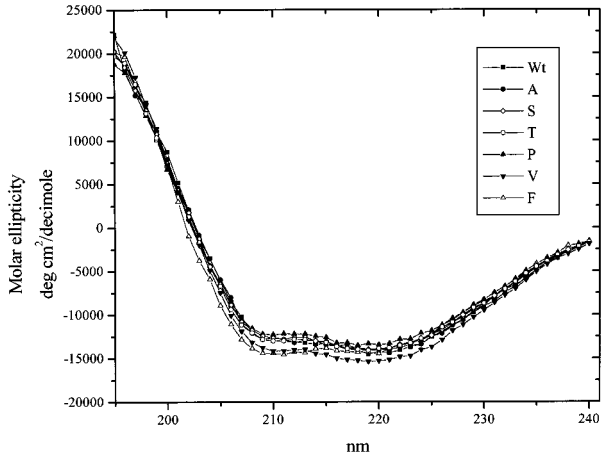

FIGURE 3: CD spectra of wild-type TbTIM, the high-activity mutants, and C14F TbTIM. The spectra of the indicated enzymes at a concentration of 100 μg/mL in phosphate buffer and 20 mM NaCl (pH 7.4) are shown.

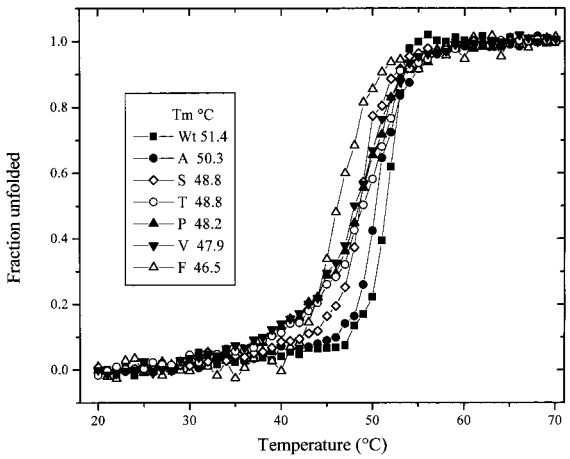

FIGURE 4: Melting curves of wild-type TbTIM, the high-activity mutants, and C14F TbTIM. The changes in molar ellipticity induced by the progressive increase in temperature were followed at 222 nm. The inset shows the T_m values of the indicated enzymes.

behavior precluded the measurements of their kinetic constants under steady-state conditions, and most probably indicates that dimeric C14G and C14N TbTIMs have low association constants. A similar phenomenon has been reported for point mutation variants of TIM that have low dimer stability (*24*, *27*, *31*). In this context, it is pointed out that, because of the rapid decay of activity that occurs during the measurements, it is likely that the activities of the intact dimers are higher than those that were detected.

Methylglyoxal Formation. Relative to the isomerization reaction, the elimination reaction catalyzed by TIM (using [^{32}P]DHAP) is slow. We could only observe it under conditions in which the enzyme concentration was higher than that of the substrate (*26*). The rate of P_i elimination by the high-activity mutants was approximately the same as that of wild-type TbTIM, 1.24−3.5 M^{-1} s^{-1}. For wild-type TbTIM and the high-activity mutants, the ratio of the rate constants of the isomerization and elimination reactions, $k_e/(k_{cat}/K_m)_{DHAP}$, corresponds to less than one methylglyoxal per 10^5 turnovers. In the C14F mutant, the rate of P_i elimination was 2.8 times higher than that of TbTIM; however, its rate constant for the isomerization reaction [$(k_{cat}/K_m)_{DHAP} = 29$ M^{-1} s^{-1}] is much lower than in the wild type (2.4×10^5 M^{-1} s^{-1}). This indicates that in the C14F mutant, the energy barrier for reprotonation is higher than in the wild type with only a modest increment of the elimination reaction.

Secondary Structure and Thermal Stability of Wild-Type TbTIM, High-Activity Mutants, and C14F TbTIM. The circular dichroism spectra of wild-type TbTIM, of the high activity mutants, and of C14F TbTIM were recorded between 190 and 240 nm at 25 °C (Figure 3). Their spectra were almost identical to that of wild-type TbTIM. Hence, the different mutations did not cause gross modifications of secondary structure.

Thermal denaturation experiments of the enzymes were carried out at a concentration of 400 μg/mL in the temperature range of 20−70 °C. The process was monitored at 222 nm. The transition curves showed that the high-activity mutants exhibited ΔT_m values 1−3 °C lower than the value of 51.4 °C exhibited by the wild-type enzyme (Figure 4). C14F TbTIM was less stable; its T_m was 46.5 °C. In the presence of phosphoglycolate, the ΔT_m of C14F TbTIM increased to 50.6 °C, a value significantly lower than the value of 57 °C observed with TbTIM in the presence of phosphoglycolate (these latter spectra are not shown).

Stability to Dilution. As noted, TIMs that have an alteration in the dimer interface lose activity when they are incubated at relatively low protein concentrations. This has been ascribed to a decrease in the association constant of the dimer, which leads to loss of monomers during the process of dissociation and association (*24*, *27*, *31*). Therefore, to learn how the substitution of Cys14 for another amino acid affects the stability of the dimer, wild-type TbTIM and the

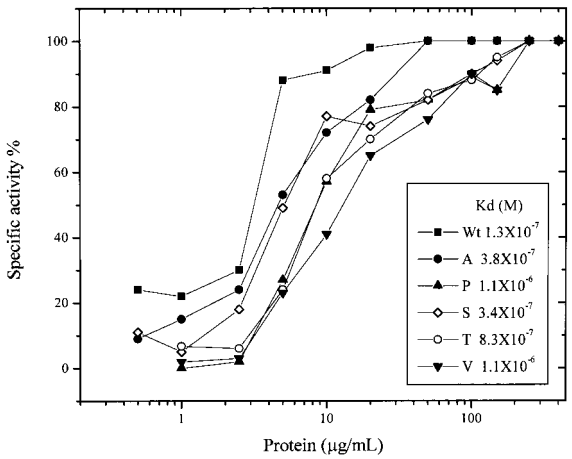

FIGURE 5: Stability of wild-type TbTIM and high-activity mutants at different protein concentrations. The enzymes were incubated at the indicated concentrations for 24 h at 25 °C in 100 mM TEA and 10 mM EDTA (pH 7.4). At that time, their activity was measured with 5 ng of protein. The respective dissociation constants (inset) were calculated as described in Materials and Methods.

high-activity mutants were incubated at different protein concentrations for 24 h. At that time, aliquots were withdrawn to measure the remaining activity with 5 ng of enzyme/mL. In the concentration range between 400 and 5 μg/mL, the activity of the wild-type remained constant. At lower protein concentrations, the activity diminished; with 0.5 μg/mL, only 20% of the original activity remained. The high-activity mutants exhibited similar inactivation patterns; however, the decay of activity occurred at higher protein concentrations (Figure 5). This was more evident with C14P, C14T, and C14V. The apparent dissociation constant (K_d) of the enzymes was calculated from these data (inset of Figure 5). For TbTIM and the C14A and C14S mutants, the K_d values were in the range of $1.3-3.8 \times 10^{-7}$ M. The C14P, C14T, and C14V mutants had higher dissociation constants. Borchert et al. (*24*, *32*) reported a K_d of 10 pM for TbTIM, which is significantly lower than the value we observed. However, there are marked differences in the experimental approaches used by those authors and us.

The inactivation that occurs during the incubation of dimeric TIMs at relatively low protein concentrations reflects the dissociation constant of the two monomers (*27*). Hence, it is relevant that the C14F mutant did not exhibit this behavior. In the concentration range from 0.5 μg/mL (the lowest concentration that could be assayed to have detectable activity) to 400 μg/mL, the activity of the enzyme did not change after its incubation for 2 h. These observations suggested that this mutant enzyme was a monomer with low, but important, catalytic activity.

Characterization of C14F TbTIM. The possibility that C14F TbTIM was a monomer was explored by size exclusion chromatography and sedimentation analysis. In the former system, the elution volumes of TbTIM (Figure 6A) corresponded to an R_s of 29.2 Å (M_r = 42 000 Da). The C14F mutant exhibited a single chromatographic peak equivalent to an R_s of 19.2 Å with an M_r of 20 000 Da. These findings are also a strong indication that C14F is a monomer.

Sedimentation analysis of C14F TbTIM was also performed. The enzyme migrated as a single symmetrical band with a sedimentation coefficient $S_{20,w}$ of 2.5044 S. This value corresponds to that of a monomeric enzyme and is in good

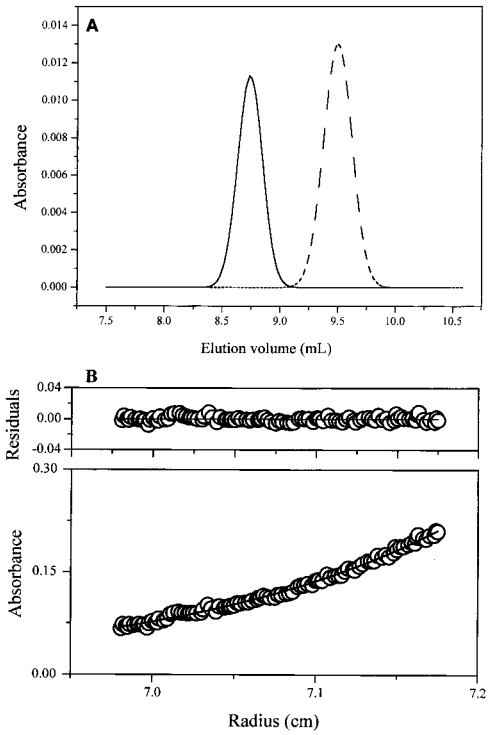

FIGURE 6: Size exclusion chromatography (A) and sedimentation equilibrium (B) of C14F TbTIM. In panel A, 100 μg of protein was injected into a UltraSpherogel-SEC 3000 column equilibrated with 100 mM TEA, 1 mM EDTA, and 150 mM NaCl (pH 7.4). The elution profile of C14F was monitored at 280 nm (dashed line). The Stokes radii were calculated from the elution volumes as described in Materials and Methods. For comparison, data for wild-type TbTIM are included (solid line). (B) Concentration distribution of C14F during sedimentation equilibrium. The empty circles are the measured values in the standard two sectors of the ultracentrifugation cell. The solid line is the result of fitting the data to a single-ideal species model using the regression analysis NONLIN program. The residual to the fit is shown at the top.

agreement with the values reported by Borchert et al. (*32*) and Schliebs et al. (*33*) for two different monomeric variants of TbTIM, 2.48 and 2.52 S, respectively. Definitive proof that C14F is a monomer was obtained from sedimentation equilibrium studies. Nonideality was not observed, and the residuals revealed no systematic deviations (Figure 6B). The NONLIN program produced a σ value of 0.95 cm^{-2}. By this method, the calculated molecular mass of C14F TbTIM was 27 200 Da, which agrees with the calculated molecular mass of the monomer of TbTIM (26 879 Da).

Taken together, the previous data indicate that C14F TbTIM is a true monomer that has a largely intact secondary structure. Thus, it was relevant to determine if this monomeric variant of TbTIM exhibits perturbations in the environment of its aromatic residues. Relative to that of TbTIM, the intrinsic fluorescence spectrum of C14F exhibited a red shift of 1.6 nm in its λ_{max} and a SCM that was ~1.8 nm higher (Figure 7A). The spectra also showed that its quantum yield was ~50% lower than in the wild-type enzyme. In accordance with these observations, the near-UV CD spectra of C14F TbTIM exhibited alterations in the environment of aromatic residues (Figure 7B). The spectral differences most likely indicate that in C14F TbTIM a buried Trp has a higher degree of solvent exposure. In this regard, a possible candidate is Trp12, since it is close to the interface Cys.

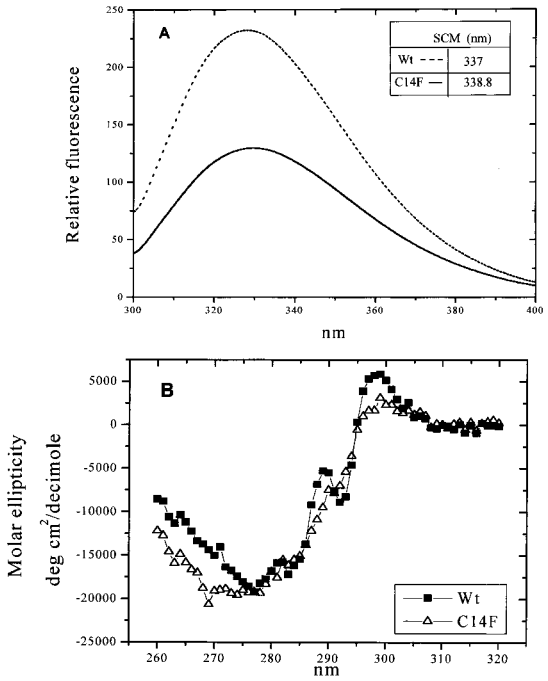

FIGURE 7: Intrinsic fluorescence emission (A) and near-UV CD (B) spectra of wild-type TbTIM and C14F. The fluorescence and CD spectra were obtained at concentrations of 0.05 and 0.4 mg/mL, respectively. The inset in panel A shows the SCM that was calculated as described in Materials and Methods.

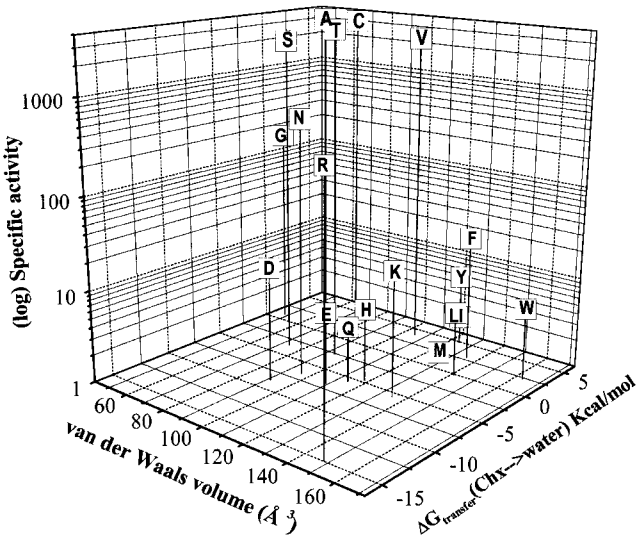

FIGURE 8: Dependence of activity of TbTIM on the van der Waals volume and polarity of the residue at position 14. The activities of wild-type TbTIM and all mutants were plotted against the van der Waals volume and polarity of the different residues. The latter is expressed as the ΔG (kilocalories per mole) of transfer from cyclohexane to water. Proline that has a van der Waals volume of 90 Å^3 was not included because it is absent in the data reported by Radzicka et al. (*35*). The amino acids are designated by the one-letter code.

DISCUSSION

Cys14 is a nonconserved residue that is at the beginning of loop 1 and forms part of the intersubunit contacts between the two monomers of TbTIM. Its side chain is completely buried within loop 3 of the other subunit (Figure 1). In the crystallographic structure of TbTIM, using an interatomic cutoff distance of 4 Å, the atoms of Cys14 contact 26 atoms of the other subunit. These numerous interactions contribute to reduce the solvent accessibility of Lys13 (loop 1) and Glu97 (loop 4) and force the main chain of catalytic residue Lys13 to adopt the strained conformation that is required for optimal catalysis (*34*). The central role of Cys14 and that of other residues at position 14 for the stability of TIM dimers is highlighted by several independent lines of research. The substitution of Cys14 with a Leu residue in TbTIM (*18*) or of Met14 in human TIM with Gln (*27*) yielded enzymes with very low stability. Likewise, several reports show that derivatization of Cys14 with sulfhydryl reagents brings about large structural changes and abolition of catalysis (*17*). In this work, we replaced Cys14 with each of the other 19 amino acids and examined how the different substitutions affect activity and stability.

From the data, it is clear that some substitutions (C14A, C14S, C14P, C14T, and C14V) do not significantly affect the catalytic activity of the enzyme. Thus, we explored if there are common features between these amino acids, and if their characteristics differ from those of the other residues that yield enzymes with low activity. Figure 8 is a plot of activity of the enzymes that have the indicated amino acid in position 14 versus their respective van der Waals volumes and polarities, the latter expressed as ΔG of transfer from a nonpolar solvent to an aqueous solution (*35*). The results show that the amino acids that yield catalytically competent enzymes fall in a van der Waals volume range between 65 and 110 Å^3, and that they have relatively low polarity. Variations of each of these two parameters give enzymes with very low activity. For example, Asn yields an enzyme with low activity; its volume is in the "allowed" range, but its polarity is high. By the same token, Gly has the right polarity, but its volume is small. Thus, these data define the physicochemical characteristics that a given residue must possess to yield a catalytically competent enzyme. It is noted that the same profile was observed when the accessible surface area was plotted instead of van der Waals volumes (not shown).

Another salient feature of the data obtained with the mutants of Cys14 is that only the high-activity mutants exhibited dissociation constants and thermal stabilities similar to those of wild-type TbTIM. This suggests that these enzymes have high activities because they conserve their dimeric structure. The relationship between dimer stability and catalysis is also illustrated by the behavior of the mutants that had "intermediate" activity (C14N, C14G, and C14R). These enzymes exhibited substantial catalytic activity in the initial seconds of reaction time. However, at the concentrations that could be used for activity measurements, their activity decreased dramatically. Hence, the overall data indicate that in TIM dimer stability is compulsorily linked to optimal catalytic activity.

In this context, the characteristics of C14F TbTIM are relevant to the question of how dimerization induces the expression of high catalytic rates. As evidenced by size exclusion chromatography and ultracentrifugation experiments, the introduction of a bulky residue in position 14 yields a monomer that exhibits catalytic activity, albeit at rates ~1000 lower than that of wild-type TbTIM. This monomeric enzyme exhibits some notable structural features. The mutant has a secondary structure that is nearly identical to that of the native dimer; however, the quantum yield of its aromatic residues is significantly lower (Figure 7A). This

indicates that the α/β folds that characterize native TbTIM can be formed in the absence of interactions with the other subunit, and that the monomer, although with alterations in the environment of its aromatic residues (Figure 7B), has, nonetheless, a tertiary structure that supports the expression of catalysis.

The existence of monomeric TIMs with catalytic activity has been previously reported (*31*−*34*, *36*). The monomeric variants of TbTIM generated either by point mutations of two conserved residues at the tip of loop 3, Thr75 and Gly76 (*33*), or by substitution of His 47 for Asn in loop 2 (*31*) exhibited catalytic constants similar to those of C14F TbTIM. The crystallographic studies of a catalytically active monomeric TIM, prepared by shortening of loop 3 (mono-TIM), showed that that the arrangements of loop 1 and 4 differed from those in wild-type TbTIM (*37*). In mono-TIM, the side chain of the catalytic Lys13 was mobile and the catalytic His95 had a different conformation. Thus, as proposed previously (*33*, *34*, *37*), it is very likely that dimerization induces the correct geometry of the catalytic residues. The lack of a correct geometry of the side chain of monomeric C14F could explain its low catalytic rates and alterations of K_m. There is also evidence that the region of the interface formed by residue 14 and loop 3 plays a dynamic role in catalysis. Gracy et al. (*38*) found that active catalysis or the occupancy of the catalytic site by a substrate analogue confers to rabbit and human TIMs a conformation prone to deamidation of an interface Asn. Likewise, it was shown that the occupancy of the catalytic site by substrate or phosphoglycolate has a strong influence on the access of thiol reagents to the interface cysteine of the TIMs from trypanosomatids (*22*). Taken together, the existing information indicates that dimerization, and in particular the interactions of residue 14 with loop 3 of the other subunit, is central to the structure and function of the enzyme.

There is another characteristic of C14F TbTIM that deserves further comment. The most extensive and obvious conformational changes that occur in TIMs during catalysis occur in loop 6 (residues 168−178). The movements of this loop and the amino acid compositions of the hinges of loop 6 have been extensively studied (*39*−*45*), and it was recently reported that the motion of loop 6 is partially rate-limiting for the chemical reaction (*46*, *47*). It is also documented that the closure of the catalytic site by loop 6 constrains the enediolate intermediate into a planar form and isolates the intermediate from bulk water (*45*). These two factors favor the isomerization reaction over the elimination reaction (formation of methylglyoxal and phosphate).

Along this line, it has been shown that a shortening of loop 6 yields an enzyme in which the partition between methylglyoxal and product formation is increased (*48*). Kinetically, it has been reported (*45*, *47*) that if the opening of loop 6 is faster than the isomerization reaction, methylglyoxal will be formed. The measurements of the rate of elimination (with [^{32}P]DHAP as the substrate) in the C14F monomers showed that the amount of $^{32}P_i$ formed was between 2 and 3 times higher than in wild-type TbTIM, although the yield of the isomerization reaction was ~1000 times lower than in the wild type. This suggests that in the monomers of C14F, the absence of intersubunit contacts influences the partition between methylgyoxal and product through an increase in the energy barriers of the reprotonation step.

In sum, the central role of the amino acid at position 14 in maintaining the dimeric structure of TIM from *T. brucei* has been confirmed. The studies also show that the amino acids that have a certain volume and polarity can successfully replace the interface cysteine. When residue 14 is replaced with amino acids that are outside the volume and polarity limits, enzymes with low stabilities are obtained. Indeed, C14F TbTIM is a monomer at a concentration of at least 400 μg/mL. The data also show that this monomeric variant of TbTIM exhibits catalytic activity. However, its kinetics of the isomerization reaction differ markedly from those of wild-type TbTIM. In addition, the monomeric enzyme exhibits alterations in the ratio between the isomerization and elimination reactions. Thus, the findings reported in the literature (*27*, *33*, *34*, *37*, *49*), together with those described here, indicate that dimerization induces the correct arrangement of the catalytic residues and that the dimer interface plays a dynamic role in the physiological function of the enzyme.

ACKNOWLEDGMENT

We thank Nallely Cabrera for excellent technical assistance and Dr. P. A. M. Michels (Research Unit for Tropical Diseases, ICP-TROP, Brussels, Belgium) for the TbTIM gene.

REFERENCES

1. Knowles, J. R. (1991) *Nature 350*, 121−124.
2. Banner, D. W., Bloomer, A. C., Petsko, G. A., Phillips, D. C., Pogson, C. I., Wilson, I. A., Cornan, P. H., Furth, A. J., Milmar, J. D., Offord, R. E., Priddle, J. D., and Waley, S. G. (1975) *Nature 255*, 609−614.
3. Lolis, E., Alber, T., Davenport, R. C., Rose, D., Hartman, F. C., and Petsko, G. (1990) *Biochemistry 29*, 6609−6618.
4. Wierenga, R. K., Noble, M. E. M., Vriend, G., Nauche, S., and Hol, W. G. J. (1991) *J. Mol. Biol. 220*, 995−1015.
5. Noble, M. E. M., Zeelen, J. P., Wierenga, R. K., Manfroid, V., Goraj, K., Gohimont, A. C., and Martial, J. A. (1993) *Acta Crystallogr. D49*, 403−417.
6. Mande, S. C., Mainfroid, V., Kalk, K. H., Goraj, K., Martial, J. A., and Hol, W. G. J. (1994) *Protein Sci. 3*, 810−821.
7. Delboni, L. F., Mande, S. C., Rentier-Delrue, F., Mainfroid, V., Turley, S., Vellieux, F. M. D., Martial, J. A., and Hol, W. G. J. (1995) *Protein Sci. 4*, 2594−2604.
8. Velanker, S. S., Ray, S. S., Gokhale, R. S., Suma, S., Balaram, H., Balaram, P., and Murthy, M. R. N. (1997) *Structure 5*, 751−761.
9. Alvarez, M., Zeelen, J. P., Mainfroid, V., Rentier-Delrue, F., Martial, J. A., Wyns, L., Wierenga, R. K., and Maes, D. (1998) *J. Biol. Chem. 273*, 2199−2206.
10. Maldonado, E., Soriano-García, M., Moreno, A., Cabrera, N., Garza-Ramos, G., Tuena de Gómez-Puyou, M., Gómez Puyou, A., and Pérez-Montfort, R. (1998) *J. Mol. Biol. 283*, 183−203.
11. Williams, J. C., Zeelen, J. P., Neubauer, G., Vried, G., Backmann, J., Michels, P. A. M., Lambeir, A. M., and Wierenga, R. K. (1999) *Protein Eng. 12*, 243−250.
12. Maes, D., Zeelen, J. P., Thanki, N., Beaucamp, N., Alvarez, M., Thi, M. H., Backmann, J., Martial, J. A., Wyns, L., Jaenicke, R., and Wierenga, R. K. (1999) *Proteins 37*, 441−453.
13. Walden, H., Bell, G. S., Russell, R. J. M., Siebers, B., Hensel, R., and Taylor, G. L. (2001) *J. Mol. Biol. 306*, 745−757.
14. Waley, S. G. (1973) *Biochem. J. 135*, 165−172.
15. Zabori, S., Rudolph, F., and Jaenicke, R. (1980) *Z. Naturforsch. 35*, 999−1004.

16. Reyes-Vivas, H., Hernández-Alcántara, G., López-Velazquez, G., Cabrera, N., Pérez-Montfort, R., Tuena de Gómez-Puyou, M., and Gómez-Puyou, A. (2001) *Biochemistry 40*, 3134−3140.
17. Garza-Ramos, G., Cabrera, N., Saavedra-Lira, E., Tuena de Gómez-Puyou, M., Ostoa-Saloma, P., Pérez-Montfort, R., and Gómez-Puyou, A. (1998) *Eur. J. Biochem. 253*, 684−691.
18. Gómez-Puyou, A., Saavedra-Lira, E., Becker, I., Zubillaga, R. A., Rojo-Domínguez, A., and Pérez-Montfort, R. (1995) *Chem. Biol. 2*, 847−855.
19. Landa, A., Rojo-Domínguez, A., Jiménez, L., Fernández-Velasco, D. A. (1997) *Eur. J. Biochem. 247*, 348−355.
20. Ranie, J., Kumar, V. P., and Balaram, H. (1993) *Mol. Biochem. Parasitol. 61*, 159−170.
21. Mowatt, M. R., Weinbach, E. C., Howard, T. C., and Nash, T. E. (1994) *Exp. Parasitol. 78*, 85−92.
22. Pérez-Montfort, R., Garza-Ramos, G., Hernández-Alcántara, G., Reyes-Vivas, H., Gao, X. G., Maldonado, E., Tuena de Gómez-Puyou, M., and Gómez-Puyou, A. (1999) *Biochemistry 38*, 4114−4120.
23. Singh, K. S., Mathial, K., Balaram, H., and Balaram, P. (2001) *FEBS Lett. 501*, 19−23.
24. Borchert, T. V., Pratt, K., Zeelen, J. P., Callens, M., Noble, M. E. M., Opperdoes, F. R., Michels, P. A. M., and Wierenga, R. K. (1993) *Eur. J. Biochem. 211*, 703−710.
25. Garza-Ramos, G., Pérez-Montfort, R., Rojo-Domínguez, A., Tuena de Gómez-Puyou, M., and Gómez-Puyou, A. (1996) *Eur. J. Biochem. 241*, 114−120.
26. Richard, J. P. (1991) *Biochemistry 30*, 4581−4585.
27. Mainfroid, V., Terpstra, P., Beauregard, M., Frére, J. M., Mande, S. C., Hol, W. G. J., Martial, J. A., and Goraj, K. (1996) *J. Mol. Biol. 257*, 441−456.
28. Ackers, G. K. (1967) *J. Biol. Chem. 242*, 3227−3228.
29. Philo, J. S. (1997) *Biophys. J. 72*, 435−444.
30. Johnson, M. L., Correia, J. J., Yphantis, D. A., and Halvorson, H. R. (1981) *Biophys. J. 36*, 572−588.
31. Borchert, T. V., Zeelen, J. P., Schliebs, W., Callens, M., Minke, W., Jaenicke, R., and Wierenga, R. K. (1995) *FEBS Lett. 367*, 315−318.
32. Borchert, T. V., Abagyan, R., Jaenicke, R., and Wierenga, R. K. (1994) *Proc. Natl. Acad. Sci. U.S.A. 91*, 1515−1518.
33. Schliebs, W., Thanki, N., Jaenicke, R., and Wierenga, R. K. (1997) *Biochemistry 36*, 9655−9662.
34. Schliebs, W., Thanki, N., Eritja, R., and Wierenga, R. K. (1996) *Protein Sci. 5*, 229−239.
35. Radzicka, A., and Wolfenden, R. (1988) *Biochemistry 27*, 1664−1670.
36. Saab-Rincón, G., Rivelino, J. V., Osuna, J., Sánchez, F., and Soberón, X. (2001) *Protein Eng. 3*, 149−155.
37. Borchert, T. V., Kishan, K. V., Zeelen, J. P., Schliebs, W., Thanki, N., Abagyan, R., Jaenicke, R., and Wierenga, R. K. (1995) *Structure 3*, 669−679.
38. Gracy, R. W., Yüksel, K. Ü., and Gómez-Puyou, A. (1995) in *Deamination and Isoaspartate Formation in Peptides and Proteins* (Aswad, D. W., Ed.) pp 133−155, CRC Press, Boca Raton, FL.
39. Albert, T., Banner, D. W., Bloomer, A. C., Petsko, G. A., Phillips, D., Rivers, P. S., and Wilson, I. A. (1981) *Philos. Trans. R. Soc. London, Ser. B 293*, 159−171.
40. Joseph, D., Petsko, G. A., and Karplus, M. (1990) *Science 249*, 1425−1428.
41. Lolis, P. J., and Petsko, G. A. (1990) *Biochemistry 29*, 6609−6618.
42. Sampson, N. S., and Knowles, J. R. (1992) *Biochemistry 31*, 8482−8487.
43. Williams, J. C., and McDermott, A. E. (1995) *Biochemistry 34*, 8309−8319.
44. Sun, J., and Sampson, N. S. (1999) *Biochemistry 38*, 11474−11481.
45. Xiang, J., Sun, J., and Sampson, N. S. (2001) *J. Mol. Biol. 307*, 1103−1112.
46. Rozovsky, S., and McDermott, A. E. (2001) *J. Mol. Biol. 310*, 259−270.
47. Rozovsky, S., Jogl, G., Tong, L., and McDermott, A. E. (2001) *J. Mol. Biol. 310*, 271−280.
48. Pompliano, D. L., Peyman, A., and Knowles, J. R. (1990) *Biochemistry 29*, 3186−3194.
49. Borchert, T. V., Abagyan, R., Kishan, K. V., Zeelen, J. P., and Wierenga, R. K. (1993) *Structure 1*, 205.

BI011950F